Multiscale model reduction methods for flow in heterogeneous porous media

Assyr Abdulle and Ondrej Budáč

Abstract. In this paper we provide a general framework for model reduction methods applied to fluid flow in porous media. Using reduced basis and numerical homogenization techniques we show that the complexity of the numerical approximation of Stokes flow in heterogeneous media can be drastically reduced. The use of such a computational framework is illustrated at several model problems such as two and three scale porous media.

1 Introduction

Fluid flow in porous media is an important and extensively studied process in various applications. Depending on the application, different model and description of a porous medium are used. One of the oldest models is the Darcy equation, which is an elliptic partial differential equation (PDE), that describes an effective fluid flow and pressure in a porous medium [12]. The porous structure, whose geometry is not present in the Darcy model, is accounted for in a permeability tensor. A more precise description is obtained by considering the porous structure explicitly. Knowledge of the geometry of the porous material allows to use a standard model of a fluid flow around obstacles. One can use the Navier-Stokes equation but also the Stokes equation, since the Reynolds number in porous media is often very small.

Let us briefly compare the aforementioned Darcy and fine scale Stokes models. To apply the Darcy model, the permeability tensor of the material is needed. It may be known for standard materials, it can sometimes be obtained experimentally, or, as we present below, it can be computed from the fine scale material structure. The fine scale Stokes approach does not need any effective material property but the computational effort of a direct numerical implementation scales with ratio between the macroscopic domain of interest and the size (typically micrometer) of the pore structure. Hence, this approach is unfeasible for fine porous structures since the number of degrees of freedom is prohibitive.

Numerical methods that combine both models and bridge the Darcy and the Stokes scale have been developed, see [2,8,10] and the references therein.

A. Abdulle · O. Budáč
École Polytechnique Fédérale de Lausanne, ANMC, CH-1015 Lausanne
e-mail: assyr.abdulle@epfl.ch; ondrej.budac@epfl.ch

The Darcy model is used on the macro scale and the effective permeability is upscaled from localized fine scale Stokes computations. This upscaling is based on the homogenization theory [16,17,7], which established that a suitable upscaling of the Stokes model leads to the Darcy model. As an example of a numerical realization of this mathematical upscaling procedure we briefly describe the *Darcy-Stokes finite element heterogeneous multiscale method* (DS-FE-HMM) that was introduced in [2]. The *finite element method* (FEM) with numerical quadrature is applied at the macro scale to discretize the Darcy equation and the permeability tensor is recovered at suitable quadrature points. Around every quadrature point we sample the microstructure of the material and solve a Stokes micro problem in a micro domain. The velocity solutions of the micro problems are then avereged to obtain an approximation of the effective permeability that is in turn used to solve the macroscopic Darcy problem. This approach avoids discretization of the whole fine scale porous structure of the material and only zooms on the microstructure where needed.

Most of the multiscale numerical methods for fluid flow in porous media are indeed two-scale, since they consider only the macroscopic (Darcy) scale and the microscopic (Stokes) scale. In practice, however, there are interesting physical processes at more than two scales, for example manufacturing of textile microstructures [13]. Such materials do not fit well into the two-scale setting and modeling that goes beyond two scales is needed. We mention for example [14,1] where multiscale methods for $n-$scale model (all of which of Darcy type) have been developed. For simplicity, we consider here three-scale models but with different physical model at each scale. The macroscopic description is again the Darcy model with a permeability recovered from a mesoscopic scale, where the fluid flow is described by the Stokes-Brinkman equation. The structure of the porous parts of the mesoscopic domains is described at an even finer scale, the microscopic scale, where the Stokes model is used. We note that the Stokes-Brinkman equation provides a simple coupling of the Stokes equation in the mesoscopic fluid part and the Darcy equation in the mesoscopic porous part. The permeability in the mesoscopic porous part is upscaled from the Stokes micro problems.

Both two-scale and three-scale numerical methods are computationally intensive since we compute a large number of local meso or micro problems ("the cell problems") that are used to upscale the permeability tensor. Errors that are committed by numerical approximation on all scales need to be balanced to obtain an efficient method. While the time cost of such coupled micro-meso-macro multiscale methods does not depend on the pore sizes, it still grows quickly while refining the macroscopic domain. One approach to reduce the computational time cost is to adaptively control the refinement on each scale, which was successfully applied in the two-scale settings [2]. Further reductions are possible by exploiting redundancy in cell problems. Model reduction techniques such as the *reduced basis* (RB) method [3] can

be applied to select only the most significant cell problems which can lead to a speed up of orders of magnitude [4].

In this paper we review two-scale and three-scale porous media and multiscale model reduction methods for fluid flow in such media. The cell problems (micro and meso) can be paramterized and formulated in a common framework that is suitable for the RB method. The main element of the RB method is an affine decomposition of the parametric problem, which needs to be provided for the cell problems. The *empirical interpolation method* (EIM) [9] is an important tool to obtain such an affine decomposition of the meso scale [5].

This paper is structured as follows. In section 2 we introduce the two- and three-scale porous media and the corresponding flow models. Numerical homogenization methods for such models are described in section 3 and the combination with model order reduction techniques is presented in section 4. Numerical experiments that illustrate the behavior of the multiscale model reduction methods are provided in section 5.

2 Multiscale porous media and flow models

Let $d \in \{2,3\}$ and $\Omega \subset \mathbb{R}^d$ be a connected bounded domain in which we consider a porous medium represented by a fluid subset $\Omega_\varepsilon \subset \Omega$, where $\varepsilon > 0$ denotes the microscopic feature scale. Fluid flow in Ω_ε can be modeled by the Stokes equation: find a velocity field $\mathbf{u}^\varepsilon$ and a pressure p^ε such that

$$\begin{aligned} -\Delta \mathbf{u}^\varepsilon + \nabla p^\varepsilon &= \mathbf{f} \quad \text{in } \Omega_\varepsilon, \\ \operatorname{div} \mathbf{u}^\varepsilon &= 0 \quad \text{in } \Omega_\varepsilon, \\ \mathbf{u}^\varepsilon &= 0 \quad \text{on } \partial\Omega_\varepsilon, \end{aligned} \tag{1}$$

where $\mathbf{f}$ is a given force field. For $\varepsilon \ll \operatorname{diam}(\Omega)$ the geometry of Ω_ε is too complex, which makes its meshing and direct numerical solution to (1) prohibitive. Instead, we examine the limit behavior of the solution $(\mathbf{u}^\varepsilon, p^\varepsilon)$ for $\varepsilon \to 0$, which is studied by the homogenization theory. An effective limit solution can be derived in various situations, in particular for periodic porous media [6,16,17] and locally periodic porous media [11,2], as follows. First, we extend the solution $(\mathbf{u}^\varepsilon, p^\varepsilon)$ from Ω_ε to Ω and denote it $(\mathbf{U}^\varepsilon, P^\varepsilon)$. Second, it can be shown that there exist a homogenized pressure p^0 and a homogenized velocity field $\mathbf{u}^0$ such that $P^\varepsilon \to p^0$ strongly in $L^2_{\mathrm{loc}}(\Omega)/\mathbb{R}$ and $\mathbf{U}^\varepsilon/\varepsilon^2 \to \mathbf{u}^0$ weakly in $L^2(\Omega)$. Finally, the homogenized pressure p^0 is shown to be a solution to the Darcy problem

$$\begin{aligned} \nabla \cdot a^0(\mathbf{f} - \nabla p^0) &= 0 \quad \text{in } \Omega, \\ a^0(\mathbf{f} - \nabla p^0) \cdot \mathbf{n} &= 0 \quad \text{on } \partial\Omega, \end{aligned} \tag{2}$$

where the effective permeability a^0 is related to the porous structure of Ω_ε as is presented below. Moreover, we have $\mathbf{u}^0 = a^0(\mathbf{f} - \nabla p^0)$.

In the next two sections we describe the two- and three-scale porous media that are illustrated in Figure 1.

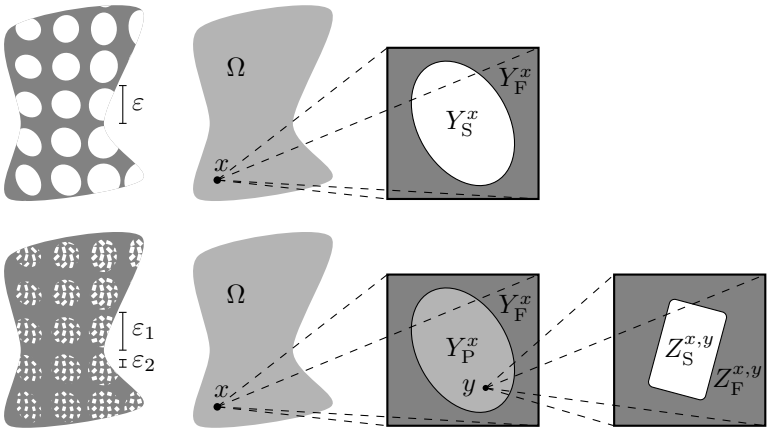

Fig. 1. The construction of Ω_ε (top) and $\Omega_{\varepsilon_1,\varepsilon_2}$ (bottom).

2.1 Two-scale porous media

We recall the definition of periodic and non-periodic two-scale porous media $\Omega_\varepsilon \subset \Omega$. Denote by Y the d-dimensional unit cube $(-1/2, 1/2)^d$, let $Y_{\mathrm{S}} \subset \overline{Y}$, and set $Y_{\mathrm{F}} = Y \backslash Y_{\mathrm{S}}$. Here and subsequently the subscripts F and S stand for the fluid and solid part, respectively. We define a two-scale periodic porous medium in Ω by $\Omega_\varepsilon = \Omega \backslash \cup_{k\in\mathbb{Z}^d} \varepsilon(k + Y_{\mathrm{S}})$. Homogenization theory requires additional assumptions on Y_{S} and Y_{F}, but they are not too restrictive. We assume that Y_{S} is closed in $\overline{Y}$, both Y_{S} and Y_{F} have positive measure. Moreover, the sets Y_{F} and $\mathbb{R}^d \backslash \cup_{k\in\mathbb{Z}^d} (k + Y_{\mathrm{S}})$ are connected, have locally Lipschitz boundaries, and are locally located on one side of their boundaries.

We define non-periodic porous media by allowing for a deformation of the reference pore geometry. Consider a continuous map $\varphi : \mathbb{R}^d \times \overline{Y} \to \overline{Y}$ such that for every $x \in \mathbb{R}^d$ the function $\varphi(x, \cdot) : \overline{Y} \to \overline{Y}$ is a homeomorphism with $\varphi(x, \cdot), \varphi(x, \cdot)^{-1} \in W^{1,\infty}(Y)$. For any $x \in \Omega$ we define the local porous geometry as $Y_{\mathrm{S}}^x = \varphi(x, Y_{\mathrm{S}})$ and $Y_{\mathrm{F}}^x = Y \backslash Y_{\mathrm{S}}^x$. We define a non-periodic two-scale porous medium by

$$\Omega_\varepsilon = \Omega \backslash \cup_{k\in\mathbb{Z}^d} \varepsilon(k + Y_{\mathrm{S}}^{\epsilon k}).$$

In the two-scale setting the homogenization theory relates the local porous geometry $(Y_{\mathrm{F}}^x, Y_{\mathrm{S}}^x)$ to the effective permeability as follows. For any point $x \in \Omega$ and $i \in \{1, \dots, d\}$ we solve the Stokes micro problem: find the velocity field $\mathbf{u}^{i,x}$ and pressure $p^{i,x}$ such that

$$\begin{aligned} -\Delta \mathbf{u}^{i,x} + \nabla p^{i,x} &= \mathbf{e}^i \quad \text{in } Y_{\mathrm{F}}^x, & \mathbf{u}^{i,x} &= 0 \quad \text{on } \partial Y_{\mathrm{S}}^x, \\ \operatorname{div} \mathbf{u}^{i,x} &= 0 \quad \text{in } Y_{\mathrm{F}}^x, & \mathbf{u}^{i,x} \text{ and } p^{i,x} &\quad \text{are } Y\text{-periodic}, \end{aligned} \tag{3}$$

where $\mathbf{e}^i$ is the i-th canonical basis vector in $\mathbb{R}^d$. We then define

$$a^0_{ij}(x) = \int_{Y^x_{\mathrm{F}}} \mathbf{e}^i \cdot \mathbf{u}^{j,x} \,\mathrm{d}y \qquad \forall i,j \in \{1,\dots,d\}. \tag{4}$$

An explicit expression for $a^0(x)$ is generally unknown and must therefore be computed numerically using (3) and (4).

2.2 Three-scale porous media

We consider porous media with a characteristic geometry at two different scales ε_1 and ε_2, where $\varepsilon_1 \gg \varepsilon_2 > 0$. If we apply the two-scale framework with $\varepsilon = \varepsilon_1$, parts of the micro domains Y^x_{F} will contain a characteristic geometry at scale $\varepsilon_2/\varepsilon_1 \ll 1$. In other words, a part (or whole) of Y^x_{F} can be considered as a porous medium with pores at scale $\varepsilon_2/\varepsilon_1$. In this situation, a direct numerical approximation of the micro problems (3) can become very costly, if not impossible.

We now embark in defining a three-scale porous medium $\Omega_{\varepsilon_1,\varepsilon_2} \subset \Omega$. Let us start with the description of the meso scale. Let $Y_{\mathrm{P}} \subset \overline{Y}$ and $Y_{\mathrm{F}} = Y \backslash Y_{\mathrm{P}}$, where P stands for porous part. We call $(Y_{\mathrm{F}}, Y_{\mathrm{P}})$ the reference mesoscopic geometry. To provide a variation at the meso scale we consider a continuous map $\varphi_1 : \mathbb{R}^d \times \overline{Y} \to \overline{Y}$ with the same properties as the map φ defined for two-scale porous media. For any $x \in \Omega$ we define the local mesoscopic geometry as $Y^x_{\mathrm{P}} = \varphi_1(x, Y_{\mathrm{P}})$ and $Y^x_{\mathrm{F}} = Y \backslash Y^x_{\mathrm{P}}$.

The porous structure of Y^x_{P} is described by the micro scale. Consider a continuous map $\varphi_2 : \mathbb{R}^d \times \mathbb{R}^d \times \overline{Y} \to \overline{Y}$ such that for every $x, y \in \mathbb{R}^d$ the map $\varphi_2(x,y,\cdot) : \overline{Y} \to \overline{Y}$ is a homeomorphism such that $\varphi_2(x,y,\cdot), \varphi_2(x,y,\cdot)^{-1} \in W^{1,\infty}(Y)$. Since we often fix parameters x and y, we simplify the notation by denoting a pair of x and y simply as $s = (x,y)$. That is, we can write $\varphi_2(x,y,z) \equiv \varphi_2(s,z)$. Let $Z_{\mathrm{S}} \subset \overline{Y}$ and $Z_{\mathrm{F}} = Y \backslash Z_{\mathrm{S}}$ be the miroscopic reference porous geometry. For any $s \in \mathbb{R}^d \times \mathbb{R}^d$ we define the local microscopic geometry as $Z^s_{\mathrm{S}} = \varphi_2(s, Y_{\mathrm{S}})$ and $Z^s_{\mathrm{F}} = Y \backslash Z^s_{\mathrm{S}}$.

For any $x \in \Omega$ we have now two different ways to view the local porous structure at x. First, we have the local mesoscopic geometry $(Y^x_{\mathrm{F}}, Y^x_{\mathrm{P}})$. Second, we can use the micro structure to define a fine scale description

$$\tilde{Y}^x_{\mathrm{S}} = Y^x_{\mathrm{P}} \backslash \cup_{k \in \mathbb{Z}^d} (\varepsilon_2/\varepsilon_1)(k + Z^{x,\varepsilon_2 k/\varepsilon_1}_{\mathrm{S}}), \qquad \tilde{Y}^x_{\mathrm{F}} = Y \backslash \tilde{Y}^x_{\mathrm{S}}.$$

Notice that $Y^x_{\mathrm{F}} \cup Y^x_{\mathrm{P}} = \tilde{Y}^x_{\mathrm{F}} \cup \tilde{Y}^x_{\mathrm{S}}$ and $\tilde{Y}^x_{\mathrm{S}} \subset Y^x_{\mathrm{P}}$ hence $Y^x_{\mathrm{F}} \subset \tilde{Y}^x_{\mathrm{F}}$. We define a three-scale porous medium in Ω by

$$\Omega_{\varepsilon_1,\varepsilon_2} = \Omega \backslash \cup_{k \in \mathbb{Z}^d} \varepsilon_1 (k + \tilde{Y}^{\varepsilon_1 k}_{\mathrm{S}}).$$

A fluid flow in $\Omega_{\varepsilon_1,\varepsilon_2}$ can be modeled by the Stokes equation as in (1). If we apply a two-scale numerical method to the three-scale medium, we will

need to solve the Stokes micro problems (3) in the domains $\tilde{Y}_{\mathrm{F}}^x$, that is: find the velocity field $\tilde{\mathbf{u}}^{i,x}$ and pressure $\tilde{p}^{i,x}$ such that

$$\begin{aligned} -\Delta\tilde{\mathbf{u}}^{i,x} + \nabla\tilde{p}^{i,x} &= \mathbf{e}^i \quad \text{in } \tilde{Y}_{\mathrm{F}}^x, & \tilde{\mathbf{u}}^{i,x} &= 0 \quad \text{on } \partial\tilde{Y}_{\mathrm{S}}^x, \\ \operatorname{div}\tilde{\mathbf{u}}^{i,x} &= 0 \quad \text{in } \tilde{Y}_{\mathrm{F}}^x, & \tilde{\mathbf{u}}^{i,x} \text{ and } \tilde{p}^{i,x} &\quad \text{are } Y\text{-periodic.} \end{aligned} \tag{5}$$

As we mentioned, a direct numerical solution to (5) might be infeasible due to the complexity of $\tilde{Y}_{\mathrm{F}}^x$. We overcome this issue by an approximation to (5) using again a homogenization-based approach. As a first attempt, one can try applying the Stokes model in the fluid part Y_{F}^x and the Darcy model in the porous part Y_{P}^x. The permeability at any $y \in Y_{\mathrm{P}}^x$ can be upscaled from the micro geometry $Z_{\mathrm{F}}^{x,y}$. However, the Stokes and Darcy models would need to be coupled at the interface of Y_{F}^x and Y_{P}^x. Such couplings, for example the Beavers–Joseph interface conditions, are non-trivial due to different orders of the models. We prefer a different approach that avoids interface conditions completely by using the Stokes–Brinkman equation at the mesocopic level. We thus consider the following mesoscopic problem: for any $x \in \Omega$ and $i \in \{1, \dots, d\}$ find the velocity $\mathbf{u}^{i,x}$ and pressure $p^{i,x}$ such that

$$\begin{aligned} -\Delta\mathbf{u}^{i,x} + \nabla p^{i,x} + K^0\mathbf{u}^{i,x} &= \mathbf{e}^i \quad \text{in } Y, & \mathbf{u}^{i,x}, p^{i,x} &\quad \text{are } Y\text{-periodic,} \\ \operatorname{div}\mathbf{u}^{i,x} &= 0 \quad \text{in } Y, \end{aligned} \tag{6}$$

where

$$K^0(x,y) = \begin{cases} (\varepsilon_1/\varepsilon_2)^2 b^0(x,y)^{-1} & \text{if } y \in Y_{\mathrm{P}}^x \\ 0 & \text{otherwise.} \end{cases}$$

and the microscopic permeability $b^0(x,y)$ is defined below in (9). We set

$$a_{ij}^0(x) = \int_Y \mathbf{e}^i \cdot \mathbf{u}^{j,x} \,\mathrm{d}y, \qquad \forall i,j \in \{1,\dots,d\}. \tag{7}$$

The micro permeability tensor $b^0 : \Omega \times Y \to \mathbb{R}^{d\times d}$ depends on the micro porous structure. For any $s = (x,y) \in \Omega \times Y$ we can compute $b^0(s) = b^0(x,y)$ by solving the Stokes micro problems

$$\begin{aligned} -\Delta\mathbf{u}^{i,s} + \nabla p^{i,s} &= \mathbf{e}^i \quad \text{in } Z_{\mathrm{F}}^s, & \mathbf{u}^{i,s} &= 0 \quad \text{on } \partial Z_{\mathrm{S}}^s, \\ \operatorname{div}\mathbf{u}^{i,s} &= 0 \quad \text{in } Z_{\mathrm{F}}^s, & \mathbf{u}^{i,s} \text{ and } p^{i,s} &\quad \text{are } Y\text{-periodic} \end{aligned} \tag{8}$$

for the velocity $\mathbf{u}^{i,s}$ and pressure $p^{i,s}$, where $i \in \{1,\dots,d\}$ and define

$$b_{ij}^0(s) = b_{ij}^0(x,y) = \int_{Y_{\mathrm{F}}^x} \mathbf{e}^i \cdot \mathbf{u}^{j,s} \,\mathrm{d}y \qquad \forall i,j \in \{1,\dots,d\}. \tag{9}$$

We have seen a two-scale and a three-scale model problem. In the two-scale problem we use the macroscopic Darcy model (2) and the microscopic Stokes model (3) with the effective permeability (4). In the three-scale problem we use the macroscopic Darcy model (2), the mesoscopic Stokes-Brinkman model (6), and the microscopic Stokes model (8) with the effective permeabilities (7) and (9).

3 Numerical multiscale methods

We briefly describe here the numerical multiscale methods developed in [2] to solve the model problems from section 2. We start with the macro scale discretization, which is the same for both methods. In section 3.1 we outline the discretization of the micro and meso problems, which are collectively called *cell problems*. A common framework to work with all cell problems is presented in section 3.2.

Let $\{\mathcal{T}_H\}$ be a family of conformal, shape-regular triangulations of Ω parametrized by the mesh size $H = \max_{K\in\mathcal{T}_H} \operatorname{diam}(K)$. We consider the macro finite element space $S^l(\mathcal{T}_H)$ of degree $l \in \mathbb{N}$ given by

$$S^l(\mathcal{T}_H) = \{q \in H^1(\Omega);\ q|_K \in \mathcal{P}^l(K),\ \forall K \in \mathcal{T}_H\},$$

where $\mathcal{P}^l(K)$ is the space of polynomials of total degree l in element K. For every $K \in \mathcal{T}_H$ we consider a quadrature formula $(x_{K_j}, \omega_{K_j})_{j=1,\dots,J_{\mathrm{mac}}}$ with integration points $x_{K_j} \in K$ and positive weights ω_{K_j}. To achieve the optimal order of accuracy we assume that $\int_K q(x)\,\mathrm{d}x = \sum_{j=1}^{J_{\mathrm{mac}}} \omega_{K_j} q(x_{K_j})$ for any $q \in \mathcal{P}^{l'}(K)$, where $l' = \max(2l-2, l)$. A direct application of the FE method to (2) reads as follows: find $p^H \in S^l(\mathcal{T}_H)/\mathbb{R}$ such that

$$B_H(p^H, q^H) = L_H(q^H) \qquad \forall q^H \in S^l(\mathcal{T}_H)/\mathbb{R},$$

where the discrete macro bilinear form and right-hand side are given by

$$\begin{aligned} B_H(p^H, q^H) &= \sum_{K\in\mathcal{T}_H} \sum_{j=1}^{J_{\mathrm{mac}}} \omega_{K_j} a^{h_1}(x_{K_j}) \nabla p^H(x_{K_j}) \cdot \nabla q^H(x_{K_j}), \\ L_H(q^H) &= \sum_{K\in\mathcal{T}_H} \sum_{j=1}^{J_{\mathrm{mac}}} \omega_{K_j} a^{h_1}(x_{K_j}) \mathbf{f}(x_{K_j}) \cdot \nabla q^H(x_{K_j}). \end{aligned} \tag{10}$$

The tensor a^{h_1} that appears in (10) is a numerical approximation of a^0 from (7) if we are in the three-scale settings. We use the tensor a^h (a numerical approximation of (4)) if we are in a two-scale setting.

3.1 Cell problems transformation and discretization

We recall that by cell problems we mean either

- the mesoscopic problem in the three-scale method (6), (7),
- the microscopic problem in the three-scale method (8), (9),
- or the microscopic problem in the two-scale method (3), (4).

The cell problems share many similarities. First, the unknowns are always velocity and pressure. Stable FE discretization for such problems are well-known and we will pick the Taylor–Hood finite element pairs. Second, the pressure is unique only up to an additive constant. Third, the velocity fields are always integrated to obtain an effective parameter for the coarser scale, see (7), (4), (9). To discretize any cell problem we proceed in several steps.

1. A weak formulation is obtained with the help of a Lagrange multiplier to normalize the pressure in order to obtain a unique solution in finite element spaces of periodic functions.
2. A change of variables is performed to map the physical sampling domain to the reference domain (such as Y_{F} or Z_{F}).
3. A Taylor–Hood FE pair is used to discretize the problem.
4. A quadrature formula is used if permeability data need to be upscaled from a finer scale (this applies to the meso scale problem, where an approximation to b^0 will be evaluated only at quadrature points in Y_{P}).
5. A discrete approximation of the permeability to be upscaled is defined.

We briefly discuss the method developed in [5] for the meso scale problem (6) in the three-scale method and refer reader to [4] for a detailed description of the micro problems. The weak formulation of (6) with a Lagrange multiplier to normalize the pressure reads as follows: for any $x \in \Omega$ and $i \in \{1, \dots, d\}$ find a velocity field $\mathbf{u}^{i,x} \in H^1_{\mathrm{per}}(Y)^d$, a pressure $p^{i,x} \in L_2(Y)$, and a Lagrange multiplier $\lambda^{i,x} \in \mathbb{R}$ such that

$$\begin{aligned}
\int_Y \Big(\sum_{j=1}^{d} \nabla \mathbf{u}_j^{i,x} \cdot \nabla \mathbf{v}_j - p^{i,x} \mathrm{div}\, \mathbf{v} \Big) \,\mathrm{d}y & \\
+ \int_Y K^0(x,y) \mathbf{u}^{i,x} \cdot \mathbf{v} \,\mathrm{d}y = \int_Y \mathbf{e}^i \cdot \mathbf{v} \,\mathrm{d}y & \qquad \forall \mathbf{v} \in H^1_{\mathrm{per}}(Y), \\
\int_Y (-q \mathrm{div}\, \mathbf{u}^{i,x} + \lambda^{i,x} q) \,\mathrm{d}y = 0 & \qquad \forall q \in L_2(Y), \\
\int_Y \kappa p^{i,x} \,\mathrm{d}y = 0 & \qquad \forall \kappa \in \mathbb{R},
\end{aligned} \tag{11}$$

where the space $H^1_{\mathrm{per}}(Y)$ consists of Y-periodic functions from $H^1(Y)$. We map the problem (11) into the reference meso structure $(Y_{\mathrm{F}}, Y_{\mathrm{P}})$ by applying the change of variables $y_{\mathrm{old}} = \varphi_1(x, y_{\mathrm{new}})$. Next, we sum the three equations into one to obtain a compact form that acts in $X_{\mathrm{mes}} = H^1_{\mathrm{per}}(Y) \times L_2(Y) \times \mathbb{R}$. The resulting problem, which is symmetric and non-coercive, and the output of interest a^0 (see (7)) are given by: find $\mathbf{U}^{i,x} \in X_{\mathrm{mes}}$ such that

$$A_{\mathrm{mes}}(\mathbf{U}^{i,x}, \mathbf{V}; x) = G^i_{\mathrm{mes}}(\mathbf{V}; x) \qquad \forall \mathbf{V} \in X_{\mathrm{mes}}, \tag{12}$$

$$a^0_{ij}(x) = G^i_{\mathrm{mes}}(\mathbf{U}^{j,x}; x) \qquad \forall i, j \in \{1, \dots, d\}. \tag{13}$$

where the bilinear form $A_{\mathrm{mes}}(\cdot, \cdot; x) : X_{\mathrm{mes}} \times X_{\mathrm{mes}} \to \mathbb{R}$ and the right-hand side $G^i_{\mathrm{mes}}(\cdot; x) : X_{\mathrm{mes}} \to \mathbb{R}$ contain integral terms with coefficients that depend on the Jacobian $\nabla_y \varphi_1(x, y)$.

We now discretize the problem (12). Let $\mathcal{T}_{h_1}$ be a conformal, shape-regular triangulation of Y, where $h_1 = \max_{K \in \mathcal{T}_{h_1}} \mathrm{diam}(K)$. We assume that for every $K \in \mathcal{T}_{h_1}$ we have either $K \subset Y_{\mathrm{F}}$ or $K \subset Y_{\mathrm{P}}$. Let $k \in \mathbb{N}$ and define the Taylor-

Hood $\mathbb{P}^{k+1}/\mathbb{P}^k$ FE spaces given by

$$\begin{aligned} V_{\text{mes}}^{h_1} &= \{\mathbf{v} \in S^{k+1}(\mathcal{T}_{h_1})^d; \quad \mathbf{v} \text{ is } Y\text{-periodic}\}, \\ P_{\text{mes}}^{h_1} &= \{q \in S^k(\mathcal{T}_{h_1}); \qquad q \text{ is } Y\text{-periodic}\}. \end{aligned}$$

Let $X_{\text{mes}}^{h_1} = V_{\text{mes}}^{h_1} \times P_{\text{mes}}^{h_1} \times \mathbb{R} \subset X_{\text{mes}}$. For every $K \in \mathcal{T}_{h_1}$ we consider a quadrature formula $(y_{K_j}, \omega_{K_j})_{j=1,\dots,J_{\text{mes}}}$ with integration points $y_{K_j} \in K$ and positive weights ω_{K_j}. An optimal order of accuracy is achieved if $\int_K q(y)\,\mathrm{d}y = \sum_{j=1}^{J_{\text{mes}}} \omega_{K_j} q(y_{K_j})$ for any $q \in \mathcal{P}^{2(k+1)}(K)$. A discretization of (12) then reads: For any $x \in \Omega$ and $i \in \{1,\dots,d\}$ find $\mathbf{U}_{h_1}^{i,x} \in X_{\text{mes}}^{h_1}$ such that

$$\begin{aligned} A_{\text{mes}}^{h_1}(\mathbf{U}_{h_1}^{i,x}, \mathbf{V}; x) &= G_{\text{mes}}^i(\mathbf{V}; x) && \forall \mathbf{V} \in X_{\text{mes}}^{h_1}, \\ a_{ij}^{h_1}(x) &= G_{\text{mes}}^i(\mathbf{U}_{h_1}^{j,x}; x) && \forall i,j \in \{1,\dots,d\}, \end{aligned} \tag{14}$$

where

$$\begin{aligned} &A_{\text{mes}}^{h_1}(\mathbf{U}, \mathbf{V}; x) = A_{\text{mes}}^{h_1}((\mathbf{u}, p, \lambda), (\mathbf{v}, q, \kappa); x) \\ &\quad = \sum_{K \in \mathcal{T}_{h_1} \cap Y_{\text{P}}} \sum_{j=1}^{J_{\text{mes}}} \omega_{K_j} \frac{{\varepsilon_1}^2}{{\varepsilon_2}^2} (b^{h_2}(x, \varphi_1(x, y_{K_j})))^{-1} \mathbf{u}(y_{K_j}) \cdot \mathbf{v}(y_{K_j})\,\mathrm{d}y \\ &\qquad + \int_Y \sum_{i,j=1}^{d} \Big(\rho_{ij}(x,y) \frac{\partial \mathbf{u}}{\partial y_i} \cdot \frac{\partial \mathbf{v}}{\partial y_j} - \sigma_{ij}(x,y) \Big(\frac{\partial \mathbf{v}_i}{\partial y_j} q + \frac{\partial \mathbf{u}_i}{\partial y_j} p \Big) \Big)\,\mathrm{d}y \\ &\qquad + \int_Y \tau(x,y)(\lambda q + \kappa q)\,\mathrm{d}y, \\ &G_{\text{mes}}^i(\mathbf{V}; x) = G_{\text{mes}}^i((\mathbf{v}, q, \kappa); x) = \int_Y \tau(x,y) \mathbf{e}^i \cdot \mathbf{v}\,\mathrm{d}y, \end{aligned} \tag{15}$$

where we denote the Jacobian $J = J(x,y) = \nabla_y \varphi_1(x,y)$ and define

$$\begin{aligned} &\rho(x,y) = \det(J)((J)^\top J)^{-1}, \quad \sigma(x,y) = \det(J) J^{-\top}, \\ &\tau(x,y) = \det(J). \end{aligned} \tag{16}$$

In (15) we denoted by b^{h_2} the numerical approximation of the micro permeability b^0 defined in (9). While the formulation (15) can seem complicated, it suffices to keep in mind the compact formulation (14).

We can apply the same approach to all the cell problems. The micro problems need to be mapped to their respective micro domains (Y_{F} in the two-scale method and Z_{F} in the three-scale method). For the micro problems a quadrature formula is not required as there is not a finer scale than the micro scale. To summarize our numerical procedure we sketch both numerical multiscale methods in a diagram in Figure 2.

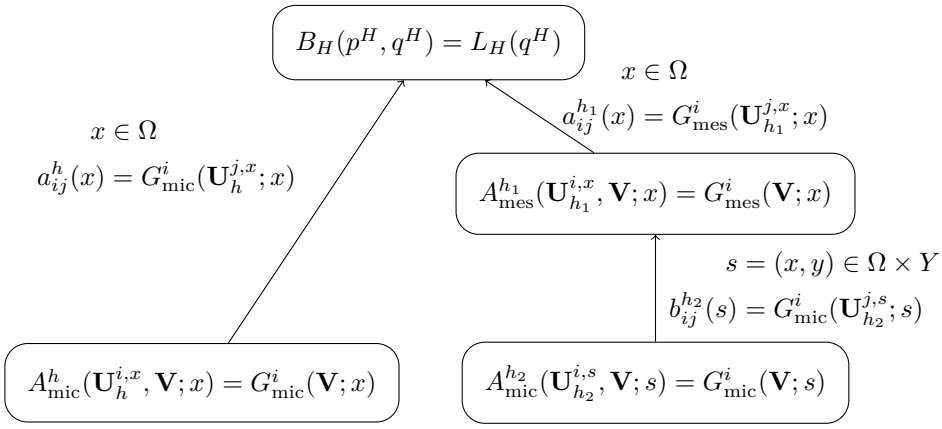

Fig. 2. A diagram of the two-scale method (left branch) and the three-scale method (right branch). Vertical direction: the Darcy macro scale (top), the Stokes-Brinkman meso scale (middle) and the Stokes micro scale (bottom).

3.2 General form of a cell problem

The various cell problems in our numerical models can be written in the following abstract form. Let $\mathcal{D}$ be parametric space of dimension at most $2d$ and X be a finite-dimensional Hilbert space. We are given a symmetric parametric bilinear form $A : X \times X \times \mathcal{D} \to \mathbb{R}$ and parametric linear forms $G^i : X \times \mathcal{D} \to \mathbb{R}$ for $i \in \{1, \dots, d\}$ with the inf-sup stability property

$$\inf_{\mathbf{U} \in X} \sup_{\mathbf{V} \in X} \frac{A(\mathbf{U}, \mathbf{V}; \mu)}{\|\mathbf{U}\|_X \|\mathbf{V}\|_X} \geq \beta(\mu) > 0 \qquad \forall \mu \in \mathcal{D}.$$

We are then interested in the evaluation of the output of interest $c : \mathcal{D} \to \mathbb{R}^{d \times d}$ that is defined via the following variational problems: for any $\mu \in \mathcal{D}$ and $i \in \{1, \dots, d\}$ find $\mathbf{U}^{i,\mu} \in X$ such that

$$A(\mathbf{U}^{i,\mu}, \mathbf{V}; \mu) = G^i(\mathbf{V}; \mu), \qquad \forall \mathbf{V} \in X \tag{17}$$

$$c_{ij}(\mu) = G^i(\mathbf{U}^{j,\mu}) \qquad \forall i, j \in \{1, \dots, d\}. \tag{18}$$

We see from Figure 2 that all cell problems can be written in the form (17), (18).

4 Model-order reduction

Both the two and the three-scale methods presented in the previous section rely on the solution of a large number of cell problems of type (17) with different parameters and the construction of an upscaled permeability (18) to be used at a coarser scale. The effective permeability depends on a parameter in $\mathcal{D} = \Omega$ or $\mathcal{D} = \Omega \times Y$ of dimension at most $2d$, where d is the physical

spatial dimension $d = 2, 3$. The repeated evaluation of the permeability for different values in $\mathcal{D}$ is a costly procedure as each evaluation relies on a PDE solve. Model order reduction can be used in this situation to build a low dimensional approximation of the solution manifold $\{\mathbf{U}^{i,\mu};\ \mu \in \mathcal{D}\}$. In or approach, we use the *reduced basis* (RB) method to construct such a low dimensional approximation space. The Petrov–Galerkin RB method [3] has been successfully applied to the two-scale problem [4] and to the three-scale problem in [5]. In section 4.1 we present an abstract version of the RB methodology and apply it to the micro scale in section 4.2 and to the meso scale in section 4.3.

4.1 Petrov–Galerkin RB method

For any $i \in \{1, \dots, d\}$ we construct a linear subspace $X_i \subset X$ that is spanned by a small number of solutions to (17). We then project (17) to the solution space X_i and a parameter-dependent test space $Y_i^\mu = T(X_i; \mu)$, where $T : X \times \mathcal{D} \to X$, called the supremizer operator, is defined below. The RB approximation of (17), (18) then reads: find $\mathbf{U}_{\mathrm{RB}}^{i,\mu} \in X_i$ such that

$$A(\mathbf{U}_{\mathrm{RB}}^{i,\mu}, \mathbf{V}; \mu) = G^i(\mathbf{V}; \mu) \qquad \forall \mathbf{V} \in Y_i^\mu. \tag{19}$$

We define a RB approximation of $c(\mu)$ with quadratic accuracy (see [15]) by

$$c_{ij}^{\mathrm{RB}}(\mu) = G^i(\mathbf{U}_{\mathrm{RB}}^{j,\mu}; \mu) + G^j(\mathbf{U}_{\mathrm{RB}}^{i,\mu}; \mu) - A(\mathbf{U}_{\mathrm{RB}}^{j,\mu}, \mathbf{U}_{\mathrm{RB}}^{i,\mu}; \mu). \tag{20}$$

For any $\mu \in \mathcal{D}$ and $\mathbf{U} \in X$ we define $T(\mathbf{U}; \mu) \in X$ as the unique element of X such that $(T(\mathbf{U}; \mu), \mathbf{V})_X = A(\mathbf{U}, \mathbf{V}; \mu)$ for every $\mathbf{V} \in X$. The supremizer operator $T(\mathbf{U}; \mu)$ is well-defined and linear in $\mathbf{U}$. Selecting Y_i^μ as the test space makes the method provably stable [3].

How do we construct a good solution space X_i? And how can we quickly evaluate (20) for any $\mu \in \mathcal{D}$? Answers to these questions rely on splitting the RB problem (19) and evaluating (20) at two different stages: an offline and an online stage.

- The *offline* stage is run only once and it is used to construct the RB space X_i and precompute necessary values for the online stage.
- The *online* stage can be run after the offline stage repeatedly and it provides a cheap and accurate approximation $c^{\mathrm{RB}}(\mu)$ for any $\mu \in \mathcal{D}$.

The RB space X_i is defined as the span of solutions $\mathbf{U}^{i,\mu}$ to (17) for a carefully selected small set of parameters $S^i \subset \mathcal{D}$, where $N_i \in \mathbb{N}$. Let us denote $(\mathbf{U}^{i,1}, \mathbf{U}^{i,2}, \dots, \mathbf{U}^{i,N_i})$ the result of applying the Gram–Schmidt orthogonalization procedure on these solutions. We thus have

$$X_i = \operatorname{span}\{\mathbf{U}^{i,1}, \mathbf{U}^{i,2}, \dots, \mathbf{U}^{i,N_i}\}.$$

The set S^i is constructed in the offline stage for every $i \in \{1, \dots, d\}$ using a greedy algorithm. Given any S_i (even empty) and a corresponding space X_i,

we can show that $\|\mathbf{U}^{i,\mu} - \mathbf{U}^{i,\mu}_{\mathrm{RB}}\|_X \leq \Delta^{\mathrm{E}}_i(\mu)$ for every parameter $\mu \in \mathcal{D}$, where the accurate a posteriori error estimator $\Delta^{\mathrm{E}}_i(\mu)$ can be evaluated cheaply for any $\mu \in \mathcal{D}$ (see [4] for details).

Algorithm: Greedy RB construction. Select a training set $\Xi \subset \mathcal{D}$ and a tolerance $\varepsilon_{\mathrm{tol}} > 0$. For each $i \in \{1, \ldots, d\}$ we start with $S^i = \emptyset$ and repeat:

1. Find $\hat{\mu} \in \Xi$ for which the value $\Delta^{\mathrm{E}}_i(\hat{\mu})$ is the largest.
2. If $\Delta^{\mathrm{E}}_i(\hat{\mu}) < \varepsilon_{\mathrm{tol}}$, we stop.
   Else, we add $\hat{\mu}$ to S^i, update the space X_i, and continue with step 1.

The offline-online splitting requires an additional assumption: existence of an affine decomposition of A and G^i. Indeed, we assume that there exist $Q_A, Q_G \ll \dim(X)$ and

- symmetric bilinear forms $A^q(\cdot,\cdot) : X \times X \to \mathbb{R}$ for $q \in \{1, \ldots, Q_A\}$,
- linear forms $G^{iq}(\cdot) : X \to \mathbb{R}$ for $q \in \{1, \ldots, Q_G\}$ and $i \in \{1, \ldots, d\}$,
- vector fields $\Theta^A : \mathcal{D} \to \mathbb{R}^{Q_A}$ and $\Theta^G : \mathcal{D} \to \mathbb{R}^{Q_G}$,

such that for any $\mathbf{U}, \mathbf{V} \in X$, parameter $\mu \in \mathcal{D}$, and $i \in \{1, \ldots, d\}$ we have

$$\begin{aligned} A(\mathbf{U}, \mathbf{V}; \mu) &= \sum\nolimits_{q=1}^{Q_A} \Theta^A_q(\mu) A^q(\mathbf{U}, \mathbf{V}), \\ G^i(\mathbf{V}; \mu) &= \sum\nolimits_{q=1}^{Q_G} \Theta^G_q(\mu) G^{iq}(\mathbf{V}). \end{aligned} \tag{21}$$

One can then apply an affine decomposition (21) in the system (19) writing the RB solution as a linear combination $\mathbf{U}^{i,\mu}_{\mathrm{RB}} \in X_i$ in the form $\mathbf{U}^{i,\mu}_{\mathrm{RB}} = \sum_{n=1}^{N_i} \alpha^{i,\mu}_n \mathbf{U}^{i,n}$, where $\alpha^{i,\mu} = (\alpha^{i,\mu}_1, \ldots, \alpha^{i,\mu}_{N_i})^T \in \mathbb{R}^{N_i}$ is a vector of unknowns. This transformation yields a dense linear system of low dimension. This linear system can be assembled in the online stage in a time cost independent of $\dim(X)$ and the computation of solution $\alpha^{i,\mu}$ is usually very fast. Thus, we can obtain $\alpha^{i,\mu}$ without reconstructing the complete RB solution $\mathbf{U}^{i,\mu}_{\mathrm{RB}}$ and use this information in (20) to compute the output of interest $c^{\mathrm{RB}}(\mu)$, again with a time cost independent of $\dim(X)$.

4.2 RB method at the micro scale

Micro problems in the two-scale and three-scale numerical methods are almost equivalent with the main difference being the parametric space. We have $\mathcal{D} = \Omega$ in the two-scale model and $\mathcal{D} = \Omega \times Y$ in the three-scale model. For simplicity of notation we consider just one of them, the three-scale model. Hence, we have a microscopic mesh size h_2, a microscopic reference mesh $\mathcal{T}_{h_2}$,

a Hilbert space $X^{h_2}_{\mathrm{mic}}$ and for any parameter $s = (x, y) \in \Omega \times Y$ we have

$$\begin{aligned} A^{h_2}_{\mathrm{mic}}(\mathbf{U}, \mathbf{V}; s) &= A^{h_2}_{\mathrm{mic}}((\mathbf{u}, p, \lambda), (\mathbf{v}, q, \kappa); s) \\ &= \int_{Z_{\mathrm{F}}} \sum_{i,j=1}^{d} \Big(\rho_{ij}(s,z) \frac{\partial \mathbf{u}}{\partial y_i} \cdot \frac{\partial \mathbf{v}}{\partial y_j} - \sigma_{ij}(s,z) \Big(\frac{\partial \mathbf{v}_i}{\partial y_j} q + \frac{\partial \mathbf{u}_i}{\partial y_j} p \Big) \Big) \, \mathrm{d}z \\ &\quad + \int_{Z_{\mathrm{F}}} \tau(s,z)(\lambda q + \kappa q) \, \mathrm{d}z, \\ G^i_{\mathrm{mic}}(\mathbf{V}; s) &= G^i_{\mathrm{mic}}((\mathbf{v}, q, \kappa); s) = \int_{Z_{\mathrm{F}}} \tau(s,z) \mathbf{e}^i \cdot \mathbf{v} \, \mathrm{d}z, \end{aligned} \tag{22}$$

where we denote the Jacobian $J = J(s,z) = \nabla_z \varphi_2(s,z)$ and define the coefficients $\rho(s,z)$, $\tau(s,z)$, and $\sigma(s,z)$ exactly as in (16). To successfully apply the RB method, we need to construct an affine decomposition (21) of the forms $A^{h_2}_{\mathrm{mic}}$ and G^i_{mic}. The main obstacle in doing so are the coefficients ρ_{ij}, σ_{ij}, and τ. If we could express them in the following affine form

$$a_1(s) b_1(z) + \cdots + a_n(s) b_n(z) \tag{23}$$

we could factor the s-dependent terms outside the integrals and an affine decomposition will be obtained. Decompositions of type (23) are not possible for arbitrary maps φ_2. However, if we assume that φ_2 is piecewise (in z) affine, then the Jacobian J will be piecewise constant, which yields a simple decomposition of type (23). Assuming that φ_2 is piecewise affine is a common practice in RB methodology for varying geometries. In case that this assumption is not valid, we can still rely on the empirical interpolation method (see section 4.3) to obtain (23) at least approximately.

4.3 RB method at the meso scale

The micro scale forms (22) and the meso scale forms (15) are very similar. They have the same terms containing ρ, τ, and σ that we dealt with in the previous section. Hence, it suffices to assume that φ_1 is piecewise affine (in y) and all but one term in (15) inherit an affine decomposition of the type (23). The only problematic term in the meso problem (15) is the term containing $b^{h_1}(x, \varphi_1(x,y))^{-1}$. Following the finding of [5] we apply the *empirical interpolation method* (EIM) [9] to obtain a decomposition

$$b^{h_1}(x, \varphi_1(x,y))^{-1} \approx a_1(x) b_1(y) + \cdots + a_n(x) b_n(y), \tag{24}$$

where the number of terms n controls the precision of the approximation. The EIM consists again of two stages: an offline stage and an online stage. The offline stage is a greedy algorithm that runs only once. The online stage allows a fast computation of the coefficients $a_1(x), a_2(x), \ldots, a_n(x)$ for any given $x \in \Omega$ by evaluating the left hand side of (24) for n selected values of y. To achieve the best performance in the three-scale method, one should combine the RB at meso and micro scale, which means that in (15) and in (24) we the tensor use b^{RB} instead of b^{h_2}.

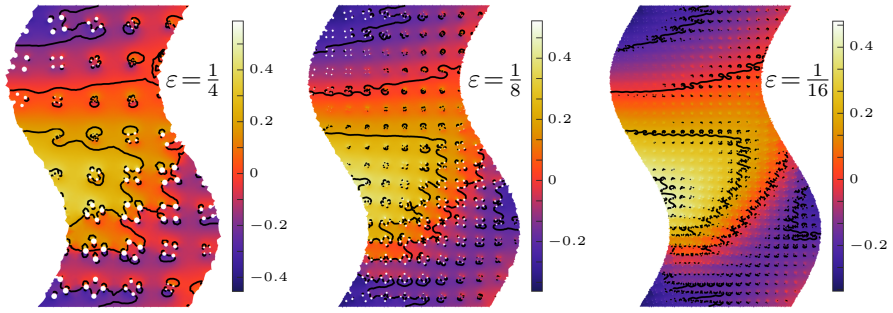

Fig. 3. Numerical approximations to the solutions p^ε to the fine scale problem (1) for $\varepsilon = 1/4, 1/8, 1/16$.

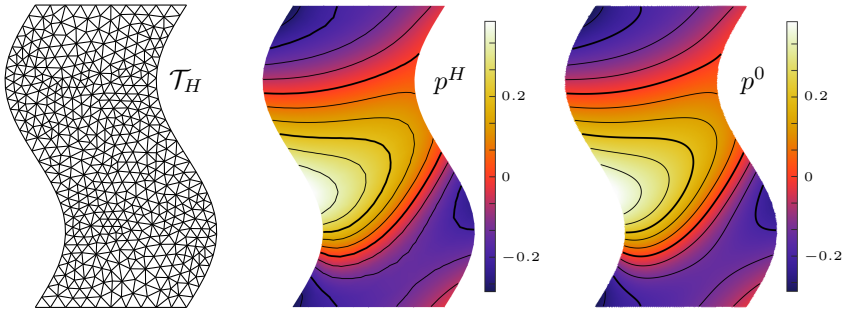

Fig. 4. Macroscopic mesh $\mathcal{T}_H$ (left), solution p^H to the reduced basis two-scale numerical method with 30 basis functions (middle), and an accurate approximation of p^0 (right).

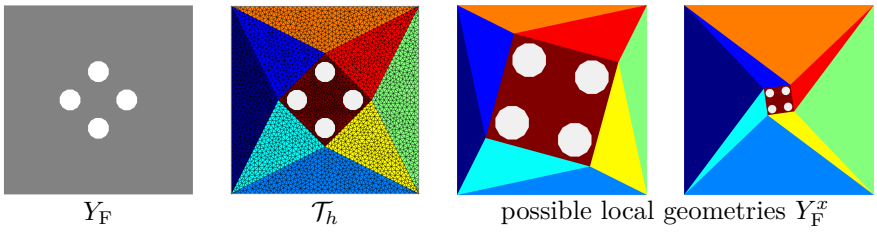

Fig. 5. From left to right: micro reference geometry Y_F, the microscopic mesh $\mathcal{T}_h$ and division of Y_F to nine subdomains, and two examples of a local porous geometry Y_F^x.

5 Numerical experiments

We illustrate the presented techniques with a two-scale numerical experiment. The code is implemented in Matlab and uses Matlab's `mldivide` to solve

dense and sparse linear systems. We use $\mathbb{P}_2/\mathbb{P}_1$ Taylor–Hood FE on the micro scale and $\mathbb{P}_1$ FE on the macro scale.

Let the macroscopic domain Ω and the initial macroscopic mesh $\mathcal{T}_H$ be as depicted in Figure 4 (left). We assume that the straight edges on the top and bottom of Ω are connected (periodic boundary conditions) and that the force field is constant with $\mathbf{f} \equiv (0, -1)$. The reference microscopic domain is depicted in Figure 5. The domain Y_{F} contains four holes that represent solid obstacles. The domain deformation function φ can rotate the four obstacles around and uniformly scale their size and position. To illustrate the range of micro geometries, two examples of the deformed micro domains Y_{F}^x are provided in Figure 5 . Moreover, we show how Y_{F} can be divided into nine parts such that φ is affine in each of them.

In Figure 3 we show the global variation of the porous structure for some (relatively large) values of ε and solutions to the fine scale problem (1). In the two-scale model we used reduced basis at the micro scale. Setting the tolerance of the greedy algorithm to $\varepsilon_{\mathrm{tol}} = 0.01$ we obtained the reduced basis of size $N_1 = N_2 = 40$. The solution p^H is depicted in Figure 4 along with a very accurate numerical reconstruction of p^0. The numerical solution p^H is in agreement with the fine scale solutions as can be seen in Figure 3.

References

1. A. Abdulle and Y. Bai, *Adaptive reduced basis finite element heterogeneous multiscale method*, Comput. Methods Appl. Mech. Engrg. **257** (2013), 201–220.
2. A. Abdulle and O. Budáč, *An adaptive finite element heterogeneous multiscale method for Stokes flow in porous media*, Multiscale Model. Simul. **13** (2015), 256–290.
3. ———, *A Petrov–Galerkin reduced basis approximation of the Stokes equation in parameterized geometries*, C. R. Math. Acad. Sci. Paris **353**:7 (2015), 641–645.
4. ———, *A reduced basis finite element heterogeneous multiscale method for Stokes flow in porous media*, accepted in Comp. Meth. Appl. Mech. Eng., 2015.
5. ———, *A three-scale offline-online numerical method for fluid flow in porous media*, preprint, 2016.
6. G. Allaire, *Homogenization of the Stokes flow in a connected porous medium*, Asymptot. Anal. **2**:3 (1989), 203–222.
7. ———, *Homogenization of the Navier-Stokes equations in open sets perforated with tiny holes i. abstract framework, a volume distribution of holes*, Arch. Ration. Mech. Anal. **113**:3 (1991), 209–259.
8. S. Alyaev, E. Keilegavlen, and J. M. Nordbotten, *Analysis of control volume heterogeneous multiscale methods for single phase flow in porous media*, Multiscale Model. Simul. **12**:1 (2014), 335–363.
9. M. Barrault, Y. Maday, N.-C. Nguyen, and A. T. Patera, *An 'empirical interpolation method': Application to efficient reduced-basis discretization of partial differential equations*, C. R. Math. Acad. Sci. Paris **339** (2004), 667–672.

10. D. L. Brown, Y. Efendiev, and V. H. Hoang, *An efficient hierarchical multiscale finite element method for Stokes equations in slowly varying media*, Multiscale Model. Simul. **11**:1 (2013), 30–58.

11. D. L. Brown, P. Popov, and Y. Efendiev, *On homogenization of Stokes flow in slowly varying media with applications to fluid-structure interaction*, GEM Int. J. Geomath. **2**:2 (2011), 281–305.

12. H. Darcy, *Les fontaines publiques de la ville de Dijon: Exposition et application á suivre et des formules á employer dans les questions de duistribution deau*, 1856.

13. M. Griebel and M. Klitz, *Homogenization and numerical simulation of flow in geometries with textile microstructures*, Multiscale Model. Simul. **8**:4 (2010), 1439–1460.

14. V. H. Hoang and C. Schwab, *High-dimensional finite elements for elliptic problems with multiple scales*, Multiscale Model. Simul. **3**:1 (2005), 168–194.

15. N. A. Pierce and M. B. Giles, *Adjoint recovery of superconvergent functionals from PDE approximations*, SIAM Rev. **42**:2 (2000), 247–264.

16. E. Sánchez-Palencia, *Non-homogeneous media and vibration theory*, Lecture Notes in Phys., vol. 127, Springer, 1980.

17. L. Tartar, Incompressible fluid flow in a porous medium—convergence of the homogenization process, ch. Appendix, pp. 368–377, Vol. 127 of Lecture Notes in Phys. [16], 1979, pp. 368–377.